Organic Electronics 62 (2018) 114–120

Contents lists available at ScienceDirect

Organic Electronics

journal homepage: www.elsevier.com/locate/orgel

Investigation of the atmosphere influence on device characteristics and NO_2 sensing performance of organic field-effect transistors consisting of polymer bulk heterojunction

Zuchong Yang[a], Shijiao Han[a,b], Yufan Liu[a], Xinming Zhuang[a], Deji Akinwande[b,*], Junsheng Yu[a,**]

[a] State Key Laboratory of Electronic Thin Films and Integrated Devices, School of Optoelectronic Science and Engineering, University of Electronic Science and Technology of China (UESTC), Chengdu, 610054, PR China

[b] Microelectronics Research Center, The University of Texas at Austin, Austin, 78758, TX, USA

ARTICLE INFO

Keywords:
Organic field-effect transistor (OFET)
Nitrogen dioxide sensor
Bulk heterojunction
Semiconducting polymer
Atmosphere influence

ABSTRACT

Organic field-effect transistors (OFETs) using polymer as the active layer are being intensively developed for flexible electronics including gas sensor. The strategy of polymer blends comprising semiconducting polymer mixed into an insulating polymer matrix has shown great potential in improving the electrical and sensing performance of OFETs. Herein two semiconducting polymers of poly(3-hexylthiophene-2,5-diyl) (P3HT) and poly(9-vinylcarbazole) (PVK) are used to construct a polymer bulk heterojunction, through exploring the atmosphere influence on device characteristics and NO_2 sensing performance of the transistors, an in-depth illumination of the underlying sensing mechanism is carried out. Firstly, by using nitrogen (N_2) and dry air as carrier gases, the individual device characteristics and sensing performance under certain NO_2 concentrations are investigated. It can be observed that O_2 has a greater effect on the electrical performance than other atmospheric components, which is different from the previous report of neat P3HT-based device. Specifically, at the high gate voltage, the response of drain current under N_2 is more than 2 times higher than that under dry air, and the mobility variation exhibits a 2-fold enhancement. In contrast, at a low gate voltage (0 V) under dry air, the response is 2-fold greater than under N_2. Then, the underlying sensing mechanism of these gas sensors consisting of various P3HT fractions in different operating environment is discussed. Finally, the OFET gas sensor with a high sensitivity to NO_2 under dry air is obtained, i.e., the highest current sensitivity is ~12381% for 15 ppm with 50% P3HT, which is more than 30 times higher than that of pure one. This study on gas sensing mechanism of OFET consisting of semiconducting polymer bulk heterojunction can offer novel inspiration to realize high performance OFET and the corresponding gas sensor.

1. Introduction

Nitrogen dioxide (NO_2), one of the most common and detrimental air pollutant oxidizing gases, is produced and released into the atmosphere from vehicles and production processing [1]. It is linked with a number of adverse effects on the respiratory system such as chronic bronchitis, emphysema and respiratory irritation at low concentrations [2,3]. Hence, the detection of this toxic gas is of great significance for our daily life. Currently, there are many commercial schemes available for NO_2 sensing, such as optical methods, which rely on the unique optical fingerprints of NO_2 gas molecules, have the highest sensitivity if ignoring their size and cost [4].

Meanwhile, OFET-based NO_2 sensors with different device architecture have achieved rapidly development [5–11]. For instance, Wang et al. reported an ultrasensitive NO_2 sensor based on 6,13-bis (triisopropylsilylethynyl) pentacene/para-sexiphenyl heterojunction, sensitivity of over 1000%/ppm together with fast response/recovery speed and a low limit of detection of 20 ppb was achieved [6]. Another typical example was reported by Huang et al., through treating the polymer-dielectric surface with UV-ozone, the sensitivity of copper phthalocyanine-based NO_2 sensor increased 50 folds for 1 ppm NO_2 [7]. Moreover, the sensing performance of OFETs can be further optimized by introducing heterojunction or hole-injection layer in organic active layer [8–11]. However, the gas-sensing layers were mostly deposited via vacuum thermal evaporation, which would limit further development in the large area, low-cost and simple application.

* Corresponding author.
** Corresponding author.
E-mail addresses: deji@ece.utexas.edu (D. Akinwande), jsyu@uestc.edu.cn (J. Yu).

https://doi.org/10.1016/j.orgel.2018.07.023
Received 23 June 2018; Received in revised form 24 July 2018; Accepted 25 July 2018
Available online 26 July 2018
1566-1199/ © 2018 Elsevier B.V. All rights reserved.

Solution processing of polymers has attracted more and more attention in the field of organic electronics [12]. However, the polymer tends to agglomerate instinctively. Hence, several approaches have been implemented in improving the polymer-film quality including choosing appropriate solvent, introducing dielectric treatment and optimizing deposition method [13]. Among them, the strategy of blending a semicondcuting polymer with an insulating polymer has recently been shown to exhibit reasonably high mobility, and often exceed the corresponding values measured in devices with pure semiconducting polymer [14,15]. Moreover, when used to fabricate the OFET gas sensor, the polymer blends can also create more interfaces to enhance the adsorption of target gas [16]. In our previous study, after blending with an insulating polymer of polystyrene (PS), the transistor with only 20% P3HT exhibited a comparable NH_3 sensing performance with that of pure one [17].

It should be noted that previous studies on high performance NO_2 gas sensors containing polymers were always electric-resistance type and realized by mixing polymer with metal-oxide nanostructure, the gas sensing performance was greatly improved due to the enhanced surface to volume ratio, where polymer only functioned as a conducting element [18,19]. Due to the depletion layer existing on the surface of metal oxides, these sensors prefer being operated at oxygen-sufficient atmosphere, and dry air was always introduced as the carrier gas to dilute NO_2 [20–22]. In contrast, compared to H_2O, when the polymer functions as the active layer of OFET, it was reported that the atmospheric O_2 had little effect on the electrical characteristics [23]. Zhou et al. recently have investigated the effect of H_2O on the recovery characteristics and the corresponding ammonia detecting mechanism of organic transistor [24]. However, until now the influence of atmosphere on NO_2 sensing performance for OFET gas sensors based on polymer bulk heterojunction consisting of two semiconducting polymers is rarely studied.

PVK can increase the interaction interface and also adsorb oxygen on the film surface like metal oxides [25]. Hence, in this work, PVK mixed with a conjugated semicoducting polymer-P3HT to construct an architecuture of bulk heterojunction is used as the active layer to fabricate OFETs by solution process. To realize high-sensitivity NO_2 detection, the OFET characteristics and sensing performance under different carrier gas atmosphere are studied by modulating the P3HT weight fractions in polymer bulk heterojunction. Then, sensing mechanism underlying the influence of operating enviroment is discussed. Finally, a highly-sensitive NO_2 gas sensor operated at the low gate voltage under dry air is obtained.

2. Experimental

2.1. Materials

P3HT (Mw > 45,000, RR = 93%) was purchased from Lumtec Corp., PVK (Mw = 1,100,000) and 1,2-dichlorobenzene were both purchased from Sigma-Aldrich. All the above materials were used as received without further purification. P3HT and PVK were dissolved in 1,2-dichlorobenzene at the same concentration of 10 mg mL^{-1} and vigorously stirred on a magnetic stirring plate overnight. Then these two solutions were mixed according to a series of preset blending ratios and consecutively stirred for 20 min to ensure sufficient mix.

2.2. Device preparation

Figure S1 depicts the schematic structure of the OFET gas sensor, which is based on a common configuration of bottom-gate, top-contact transistor. The device was processed according to the following procedure. Indium tin oxide (ITO) coated glass was used as both substrate and gate electrode. Prior to the deposition of the dielectric layers, the substrates were ultrasonically cleaned in acetone, deionized water and isopropyl alcohol in sequence. PMMA, functioned as the gate dielectric, was spin-coated on the ITO substrate at room temperature (25 °C) and baked in an oven at 90 °C for 2 h.

Subsequently, P3HT/PVK blending solutions were spin-cast onto the dielectric layer using an on-the-fly-dispensing spin-coating approach (2000 rpm) [26], in which the solution was dispensed when the spin-coater motor was already operating at a fixed rotation speed. The residual solvent was removed by drying the samples on a hot plate at 100 °C for 5 min to construct the polymer bulk heterojunction active layer. Finally, the source and drain electrodes of 50 nm gold (Au) patterned with a shadow mask were thermally evaporated on the active layer. The length and width of the conducting channel were 100 μm and 10 mm, respectively.

2.3. Film characterization and sensor test

The morphologies of films were characterized by atomic force microscopy (AFM) (Agilent, AFM 5500) in tapping mode. The inner molecular packing structure was further analysed by UV–Vis spectrophotometer (SHIMAZU UV-1700) measurements. The organic transistor sensor was stored in an airtight test chamber (approximately 2.4 mL). Dry air/N_2 and 60 ppm standard NO_2 (anhydrous) mixed at the preset concentrations was introduced into the test chamber through a mass flow controller. The electrical characteristics of all the devices were measured with a Keithley 4200-SCS Source Measure Unit under ambient conditions.

3. Results and discussion

Fig. 1 and S2 depict the transfer characteristics of OFETs with various P3HT mass fractions under different carrier gases. The electrical performance of OFETs consisting of polymer bulk heterojunction exhibits distinct variations compared with the pure one, especially the on/off ratio and drain current (I_D). In line with previous reports on semiconductor/insulator blending system, all the OFETs with bulk heterojunction show a remarkable decrease in off-state current (I_{off}) and subthreshold swing (SS), also an increase in field-effect mobility (μ) calculated in the saturation regime according to Eq. (1):

$$I_{DS} = \left(\frac{WC_i}{2L}\right)\mu(V_G - V_{th})^2 \quad (1)$$

where I_{DS} is the drain-source current, L and W are channel length and width, respectively. C_i is the capacitance per unit area of the dielectric

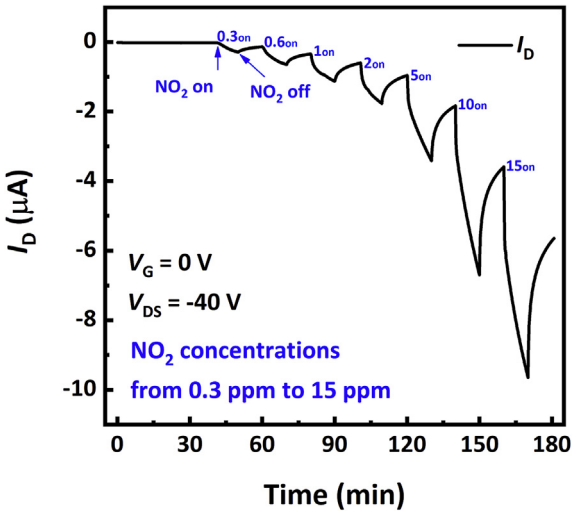

Fig. 1. Square root of drain-source current versus gate voltage plots for the indicated P3HT mass fractions at the given NO_2 concentrations with different carrier gases. (a) N_2. (b) Dry air.
(room temperature, V_{DS} = −40 V).

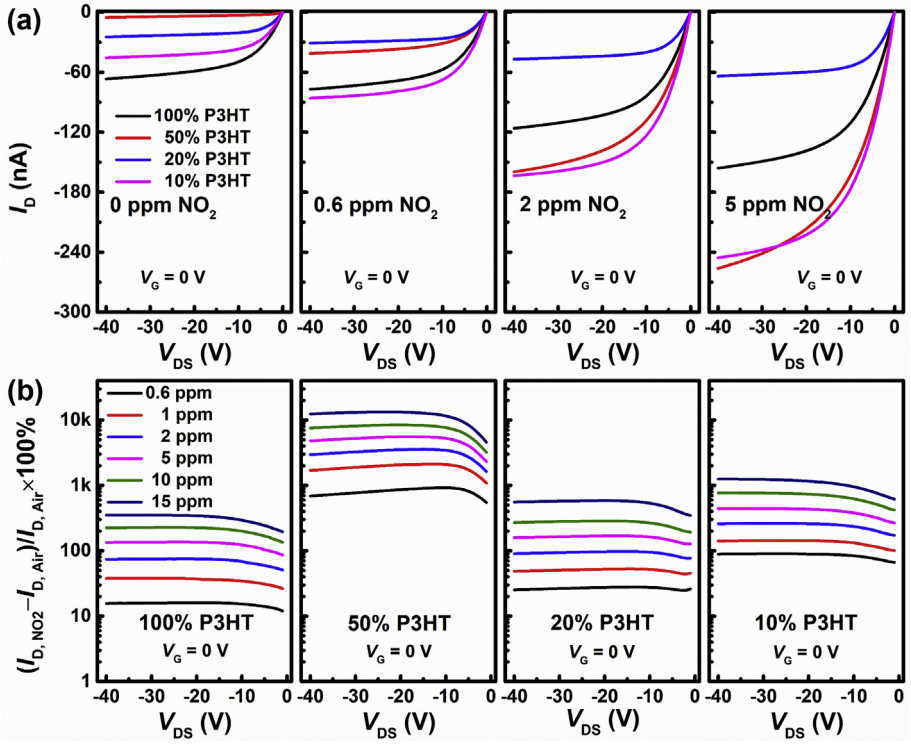

Fig. 2. Variations of I_D and μ of the indicated P3HT mass fractions at the given NO_2 concentrations with different carrier gases ($V_G = V_{DS} = -40$ V). (a) N_2, I_D. (b) Dry air, I_D. (c) N_2, μ. (d) Dry air, μ.

layer, V_G is the gate voltage, V_{th} is the threshold gate voltage.

To evaluate the NO_2 sensing performance of these OFETs under different carrier gases, they were exposed to NO_2 for 5 min in a series of concentrations ranging from 0.5 to 10 ppm with N_2 and dry air as the background atmosphere. As shown in Fig. 1 and S2, it is obvious that NO_2 sensing ability is not disrupted. Instead, all the devices with bulk heterojunction show different degrees of enhancement in response to the indicated NO_2 concentrations. Meanwhile, it should be noted that I_D shows an opposite shift when initially exposed to N_2 and dry air in the case of 50% P3HT weight fraction, and the detailed variations of electrical parameters are listed in Table S1.

Further, when the OFETs interact with various NO_2 concentrations diluted by different carrier gases, the relative changes of I_D and μ were calculated as shown in Fig. 2. The Y-axis represents the corresponding percentage change. Overall, it can be clearly observed that the maximum response comes up in the device with 50% P3HT under any carrier gas. All the devices with bulk heterojunction show much better sensing performance when using N_2 as carrier gas, which is diametrically opposed to the metal-oxide gas sensor. Upon exposure to 10 ppm NO_2, the device with 50% P3HT changes its parameters in 302% of I_D and 99% of μ under dry air atmosphere, while for the one under N_2, more significant changes in 726% of I_D and 194% of μ are observed. The NO_2 response is enhanced by a factor of ~2.4 in I_D and ~2 in μ. For the low concentration, i.e., upon exposure to 0.5 ppm NO_2, both I_D and μ increase by 2 folds than that under dry air. With a further dilution of P3HT, when the P3HT weight is 10%, the I_D change is 375% under N_2, which is almost 4 times higher than the result obtains under dry air, and μ is also enhanced by 6.5-fold.

When the device is exposed to air, oxygen molecules will be adsorbed on the surface of polymer bulk heterojunction and extract inner electrons to generate chemisorbed oxygen species such as O_2^-, as depicted in Eqs. (2) and (3). In this study, all the fresh devices were initially tested under ambient atmosphere, so oxygen would be adsorbed on the surface.

$$O_{2(gas)} \rightarrow O_{2(ads)} \quad (2)$$

$$O_{2(ads)} + e^- \rightarrow O^-_{2(ads)} \quad (3)$$

The electron affinity of NO_2 is 2.30 eV, which is much higher than that of O_2 (0.44 eV). Thus, once the device is exposed to NO_2, the NO_2 molecule could also intensively attract electrons due to its higher electrophilic property, forming adsorbed $NO^-_{2(ads)}$, and it can also react with the adsorbed oxygen. The reactions as Eqs. (4) and (5) do exist in both N_2 and dry air atmosphere. However, for the dry air atmosphere, the high O_2 concentration will inhibit these chemical reactions (Eq. (5)). As a result, the p-type doping effect of NO_2 is weakened. Hence, the device using N_2 as carrier gas can obtain higher response than dry air.

$$NO_{2(gas)} + e^- \rightarrow NO^-_{2(ads)} \quad (4)$$

$$NO_{2(gas)} + O^-_{2(ads)} \rightarrow NO^-_{2(ads)} + O_{2(ads)} \quad (5)$$

It is worth noting that this phenomenon is different from the behavior of metal oxides-based NO_2 sensor. When operated at the high gate voltage, it is possible that there may be no depletion layer induced on the surface of bulk heterojunction. Moreover, as shown in Fig. S2, the saturated drain current of device with 50% P3HT in N_2 is lower than that in dry air, which is another crucial factor for the above phenomenon since the lower intrinsic current means higher percentage change after exposing to NO_2.

Meanwhile, it can be clearly observed that I_{off} of the device with 50% P3HT measured under dry air is much lower than that under N_2 (Fig. S2). It seems to imply that when the gate voltage is low, the response may be enhanced. As depicted in Fig. 3, the response of I_D shows an obvious dependence on gate voltage. At 10 ppm NO_2, when the $V_G = 0$ V, the response under dry air is more than 10000%, which is nearly 2-fold higher than that under N_2 (~5500%). Furthermore, as shown in Fig. 3a, when increasing gate voltage from 0 V to 20 V, the response under N_2 plummeted to ~100%, which is much lower than that under dry air.

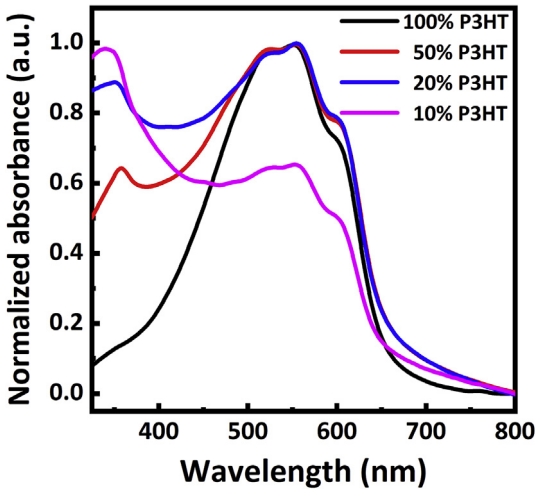

Fig. 3. I_D sensitivity - V_G plots for the indicated P3HT weight fractions and NO_2 concentrations under different atmosphere (V_{DS} = −40 V, V_G ranges from 20 V to −40 V). (a) N_2. (b) Dry air.

To explore the origin of the improving sensing performance at low gate voltage, the film morphologies were studied by AFM. Fig. 4 depicts AFM height images of the surface morphology of pure P3HT film and bulk-heterojunction films, respectively. The larger area images of 20 μm × 20 μm were summarized in Fig. S3. As revealed by these AFM height images, the surface roughness of the bulk-heterojunction films is larger than that of the pure P3HT one. Meanwhile, obvious phase separation can be observed (Fig. S3). It may be a direct consequence of the interplay between liquid-liquid demixing and stratification during the high-speed spin-coating process [27]. In particular, the morphology of the film with 50% P3HT composes of protruding globular domains (0.5–1 μm in diameter) randomly interspersed in the matrix. Based on the reported phase diagram calculation and dynamic analyzation of phase separation process, it can be primarily deduced that the bulk-heterojunction films consist of PVK rich domains in which P3HT is highly diluted and the other domains in which the semiconductor is the dominant species [28,29].

To acquire a further understanding of the inner thin film structure, UV–Vis absorption spectra were measured and demonstrated in Fig. 5. The aggregation of P3HT film can be well-characterized with its UV–Vis absorbance peaks. When the absorbance is normalized, a stronger 0-0 vibronic transition peak (at ca. 610 nm) indicates a higher conjugation length and increased planarization of the P3HT backbone [30]. As shown in Fig. 5, the 0-0 vibronic transition peak becomes stronger with the increasing weight fraction of PVK, which means that the conjugation length is gradually increasing.

Based on the above analysis of AFM and UV–Vis absorption spectroscopy, it can be observed that in the bulk heterojunction with 50% P3HT, PVK is randomly distributed among the P3HT aggregates or chains, in both horizontal and vertical directions. Since P3HT can function as an ambipolar active material [31,32], when V_G = 0 V, with V_{DS} changes from 0 V to −40 V, the presence of electron transport should not be ignored because the bias condition favours the accumulation of electrons. When exposed to dry air, PVK adsorbs oxygen molecules, according to the reaction of Eqs. (2) and (3), the oxygen will interact with the electrons. As a result, the electron resistance of bulk heterojunction increases, thus I_{off} decreases (Fig. 6a). Since the oxygen can form a charge-transfer complex with PVK [25], it can be postulated that the adsorbed oxygen form a weak depletion layer at the low gate voltage. As depicted in Fig. 6a, all the devices show similar sensing properties, the output current exhibits a gradual growth with increasing NO_2 concentrations. Although the output current of the device with 50% P3HT rises to the same level with that of 10% P3HT, it still has much higher response due to the low intrinsic current. However, with the dilution of P3HT, the conjugation length increases, in fact the sensing performance depends on the p-type doping effect on P3HT, hence even under the low gate voltage, higher response of the devices with 10% and 20% P3HT bulk heterojunction occur under N_2 atmosphere.

As the sensitivity is dependent on the gate voltage and fixed gate voltage would benefit to focusing on the conducting channel, we study the relative variation of I_D along with V_{DS} (V_G = 0 V). As shown in Fig. 6b, the response increases with V_{DS} and then becomes saturated and stable. The device with 50% P3HT needs higher V_{DS} for conducting

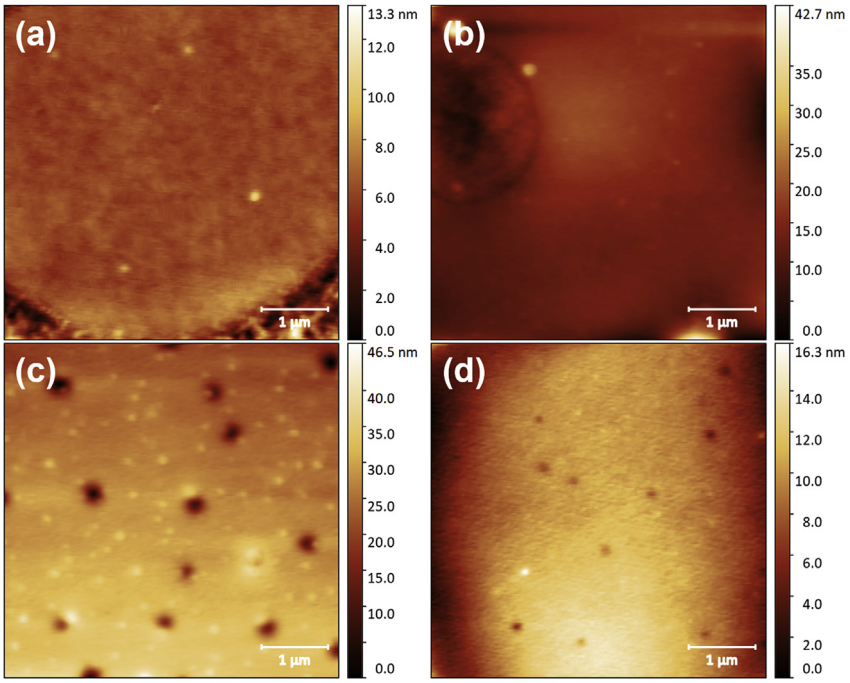

Fig. 4. AFM height images (5 μm × 5 μm) of the films with different P3HT weight fractions. (a) 100%. (b) 50%. (c) 20%. (d) 10%.

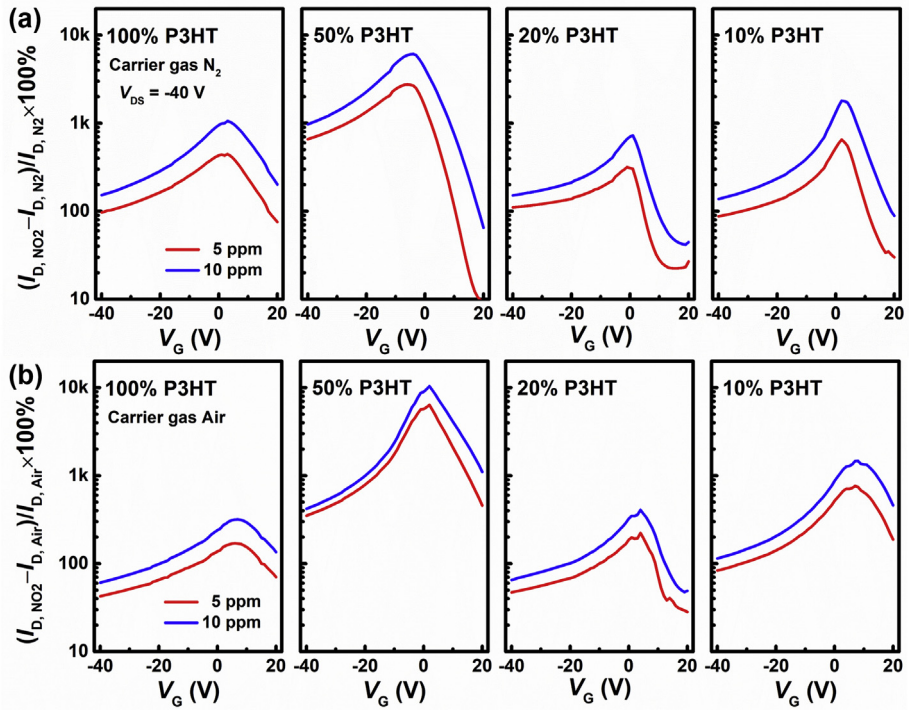

Fig. 5. Normalized UV–Vis absorption spectra of films with various P3HT mass fractions.

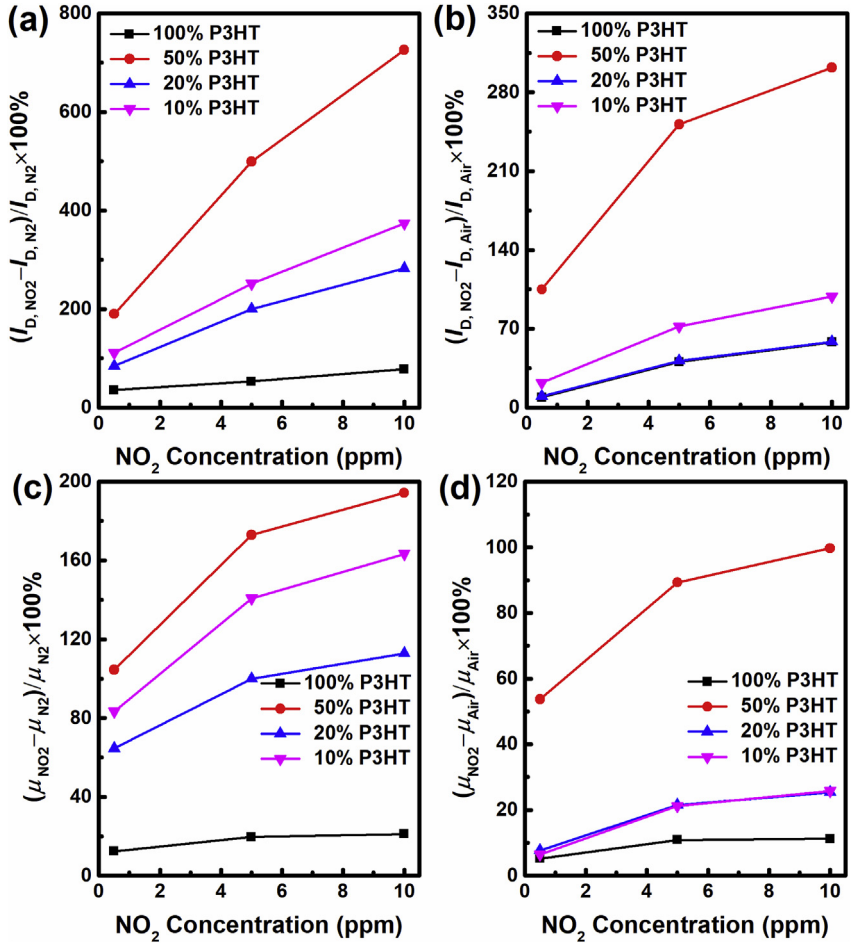

Fig. 6. (a) Output characteristics under NO_2 concentrations of 0 ppm, 0.6 ppm, 2 ppm and 5 ppm, respectively. $V_{DS} \leq 0$ V, $V_G = 0$ V. (b) Sensitivity - V_{DS} plots for the indicated P3HT weight fractions and NO_2 concentrations, $V_G = 0$ V.

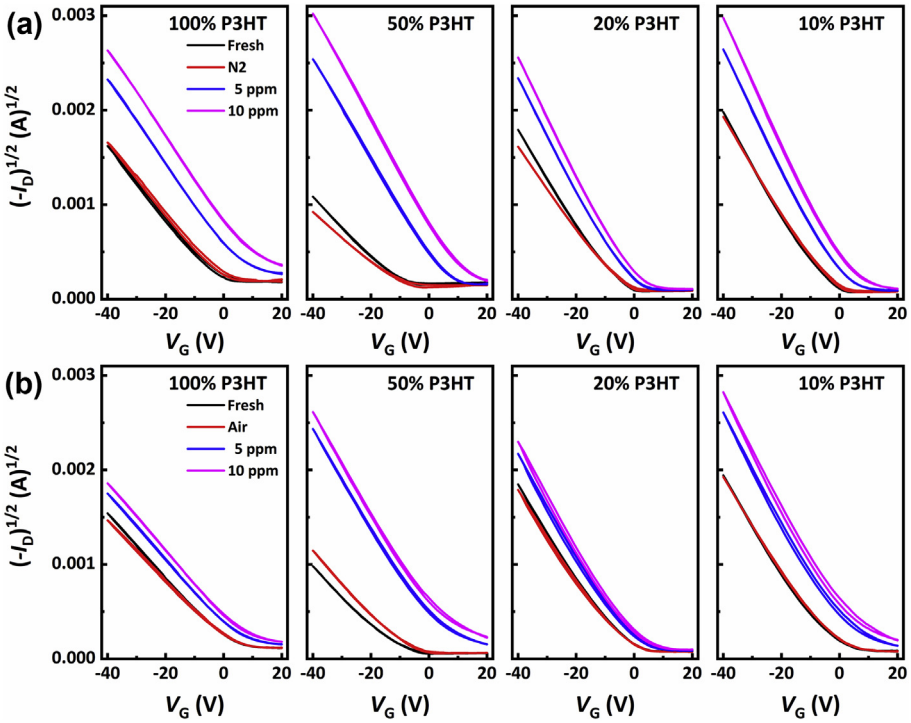

Fig. 7. Real-time response to dynamic NO_2 concentrations at room temperature. $V_G = 0$ V, $V_{DS} = -40$ V.

when $V_G = 0$ V. This can also prove that P3HT is not continuous along the horizontal direction, the charge carrier needs higher voltage to overcome the junction barrier. At $V_{DS} = -40$ V, the sensitivity of blends with 50% P3HT achieves a ~12381% increase for 15 ppm at $V_G = 0$ V, it is more than 30 times greater than that of 100% P3HT. For the low concentration detection, the device with 50% P3HT has a ~700% current gain when exposed to 0.6 ppm NO_2, while the device with 100% P3HT only displays a 16% enhancement. With a further dilution of P3HT, the responses decrease to a certain degree but still compare favourably with that of pure one. In addition, it can also be found that the sensitivity of the device with 50% P3HT reaches its detecting saturation at $V_{DS} = -10$ V, thus we suppose that this sensor may also work well with the same response at $V_{DS} = -10$ V and $V_G = 0$ V, which can greatly reduce the power consumption.

To further demonstrate the sensitivity to NO_2 with 50% P3HT using dry air as carrier gas, the real-time current response under different NO_2 concentrations was monitored as shown in Fig. 7. The device had been operated under dry air for 40 min before exposing to NO_2 to make sure I_D reached a stable status, and each NO_2 pulse kept 10 min. This dynamic test reveals that the device consisting of polymer bulk heterojunction can function regularly and can clearly distinguish NO_2 as low as 0.3 ppm.

4. Conclusion

In this work, we exploited two different carrier gases of N_2 and dry air to investigate the influence of the atmosphere on NO_2 sensing performance of OFETs consisting of polymer bulk heterojunction. For the high gate voltage, the adsorbed oxygen can weaken the response, and the drain current variation under N_2 is more than 2 times higher than that under dry air, and the mobility variation also possesses a 2-fold enhancement than the result under dry air. On the other hand, for the low gate voltage, when the P3HT weight fraction is 50%, a weak depletion layer might be induced, leading to a low intrinsic current and a 2-fold greater response. Based on the mechanism discussion, high sensitivity to NO_2 is ultimately realized, i.e., the highest current sensitivity reaches ~12381% for 15 ppm (~700% for 600 ppb) with 50% P3HT, which is more than 30 times greater than that of pure one. Even more, it can clearly distinguish NO_2 as low as 300 ppb. This study of mechanism underlying the relationship between NO_2 sensing property and operating environment will provide a valuable reference to the performance optimization of the OFET gas sensor. Additionally, the strategy of bulk heterojunction based on two semiconducting polymers, together with the advantage of simple wet-fabrication process, can offer novel inspiration to realize high performance OFET and the corresponding gas sensor.

Acknowledgement

This work was financially supported by the Foundation for Innovation Research Groups of the National Natural Science Foundation of China (Grant No. 61421002), National Key R&D Program of China (Grant 2018YFB0407100-02), and the Foundation of the NSFC (Grant Nos. 61675041 & 51703019), State Scholarship Fund of China Scholarship Council (Grant No. 201606070044).

Appendix A. Supplementary data

Supplementary data related to this article can be found at https://doi.org/10.1016/j.orgel.2018.07.023.

References

[1] S.W. Lee, W. Lee, Y. Hong, G. Lee, D.S. Yoon, Recent advances in carbon material-based NO_2 gas sensors, Sensor. Actuator. B Chem. 255 (2018) 1788–1804.
[2] G.B. Hamra, F. Laden, A.J. Cohen, O.R. Nielsen, M. Brauer, D. Loomis, Lung cancer and exposure to nitrogen dioxide and traffic: a systematic review and meta-analysis, Environ. Health Perspect. 123 (2015) 1107–1112.
[3] S.P. Holland, E.T. Mansur, N.Z. Muller, A.J. Yates, Damages and expected deaths due to excess NO_x emissions from 2009 to 2015 volkswagen diesel vehicles, Environ. Sci. Technol. 50 (2016) 1111–1117.
[4] F. Gu, L. Zhang, X. Yin, L. Tong, Polymer single-nanowire optical sensors, Nano Lett. 8 (2008) 2757–2761.
[5] W. Shi, J. Yu, H.E. Katz, Sensitive and selective pentacene-guanine field-effect transistor sensing of nitrogen dioxide and interferent vapor analytes, Sensor. Actuator. B Chem. 254 (2018) 940–948.
[6] Z. Wang, L. Huang, X. Zhu, X. Zhou, L. Chi, An ultrasensitive organic semiconductor

NO_2 sensor based on crystalline tips-pentacene films, Adv. Mater. 29 (2017) 1703192.
[7] W. Huang, X. Zhuang, F.S. Melkonyan, B. Wang, L. Zeng, G. Wang, S. Han, M.J. Bedzyk, J. Yu, T.J. Marks, A. Facchetti, UV-ozone interfacial modification in organic transistors for high-sensitivity NO_2 detection, Adv. Mater. 29 (2017) 1701706.
[8] L. Huang, Z. Wang, X. Zhu, L. Chi, Electrical gas sensors based on structured organic ultra-thin films and nanocrystals on solid state substrates, Nanoscale Horizons 1 (2016) 383–393.
[9] X. Zhuang, W. Huang, S. Han, Y. Jiang, H. Zheng, J. Yu, Interfacial modifying layer-driven high-performance organic thin-film transistors and their nitrogen dioxide gas sensors, Org. Electron. 49 (2017) 334–339.
[10] H. Fan, W. Shi, X. Yu, J. Yu, High performance nitrogen dioxide sensor based on organic field-effect transistor utilizing ultrathin CuPc/PTCDI-C8 heterojunction, Synth. Met. 211 (2016) 161–166.
[11] W. Huang, J. Yu, X. Yu, W. Shi, Polymer dielectric layer functionality in organic field-effect transistor based ammonia gas sensor, Org. Electron. 14 (2013) 3453–3459.
[12] A. Zen, J. Pflaum, S. Hirschmann, W. Zhuang, F. Jaiser, U. Asawapirom, J.P. Rabe, U. Scherf, D. Neher, Effect of molecular weight and annealing of poly(3-hexylthiophene)s on the performance of organic field-effect transistors, Adv. Funct. Mater. 14 (2004) 757–764.
[13] Y. Diao, L. Shaw, Z. Bao, S.C.B. Mannsfeld, Morphology control strategies for solution-processed organic semiconductor thin films, Energy Environ. Sci. 7 (2014) 2145–2159.
[14] L. Kergoat, N. Battaglini, L. Miozzo, B. Piro, M.C. Pham, A. Yassar, G. Horowitz, Use of poly(3-hexylthiophene)/poly(methyl methacrylate) (P3HT/PMMA) blends to improve the performance of water-gated organic field-effect transistors, Org. Electron. 12 (2011) 1253–1257.
[15] J. Smith, R. Hamilton, I. McCulloch, N.S. Stutzmann, M. Heeney, D.D.C. Bradley, T.D. Anthopoulos, Solution-processed organic transistors based on semiconducting blends, J. Mater. Chem. 20 (2010) 2562–2574.
[16] A.C. Arias, F. Endicott, R.A. Street, Surface-induced self-encapsulation of polymer thin-film transistors, Adv. Mater. 18 (2006) 2900–2904.
[17] S. Han, X. Zhuang, W. Shi, X. Yang, L. Li, J. Yu, Poly(3-hexylthiophene)/polystyrene (P3HT/PS) blends based organic field-effect transistor ammonia gas sensor, Sensor. Actuator. B Chem. 225 (2016) 10–15.
[18] T. Zhao, X. Fu, X. Cui, G. Lian, Y. Liu, S. Song, Q. Wang, K. Wang, D. Cui, An in-situ surface modification route for realizing the synergetic effect in P3HT-SnO_2 composite sensor and strikingly improving its sensing performance, Sensor. Actuator. B Chem. 241 (2017) 1210–1217.
[19] Y. Yang, H.E. Katz, Hybrid of P3HT and ZnO@GO nanostructured particles for increased NO_2 sensing response, J. Mater. Chem. C 5 (2017) 2160–2166.
[20] H. Li, J. Dailey, T. Kale, K. Besar, K. Koehler, H.E. Katz, Sensitive and selective NO_2 sensing based on alkyl- and alkylthio-thiophene polymer conductance and conductance ratio changes from differential chemical doping, ACS Appl. Mater. Interfaces 9 (2017) 20501–20507.
[21] W. Huang, P. Guo, L. Zeng, R. Li, B. Wang, G. Wang, X. Zhang, R. Chang, J. Yu, M.J. Bedzyk, Metal composition and polyethylenimine doping capacity effects on semiconducting metal oxide-polymer blend charge transport, J. Am. Chem. Soc. 140 (2018) 5457–5473.
[22] V. Saxena, D.K. Aswal, M. Kaur, S.P. Koiry, S.K. Gupta, J.V. Yakhmi, R.J. Kshirsagar, S.K. Deshpande, Enhanced NO_2 selectivity of hybrid poly(3-hexylthiophene): ZnO-nanowire thin films, Appl. Phys. Lett. 90 (2007) 043516.
[23] S. Hoshino, M. Yoshida, S. Uemura, T. Kodzasa, N. Takada, T. Kamata, K. Yase, Influence of moisture on device characteristics of polythiophene-based field-effect transistors, J. Appl. Phys. 95 (2004) 5088–5093.
[24] X. Zhou, K.F. Niu, Z. Wang, L.Z. Huang, L.F. Chi, An ammonia detecting mechanism for organic transistors as revealed by their recovery processes, Nanoscale 10 (2018) 8832–8839.
[25] J.M. Pochan, D.F. Hinman, R. Nash, Dielectric relaxation studies of poly(N-vinylcarbazole) and poly(3-chloro-N-vinylcarbazole) including the effects of sorbed oxygen, J. Appl. Phys. 46 (1975) 4115–4119.
[26] F. Zhang, C.a. Di, N. Berdunov, Y. Hu, Y. Hu, X. Gao, Q. Meng, H. Sirringhaus, D. Zhu, Ultrathin film organic transistors: precise control of semiconductor thickness via spin-coating, Adv. Mater. 25 (2013) 1401–1407.
[27] K.H. Yim, W.J. Doherty, W.R. Salaneck, C.E. Murphy, R.H. Friend, J.S. Kim, Phase-separated thin film structures for efficient polymer blend light-emitting diodes, Nano Lett. 10 (2010) 385–392.
[28] S. Coveney, N. Clarke, Pattern formation in polymer blend thin films: surface roughening couples to phase separation, Phys. Rev. Lett. 113 (2014) 5.
[29] D. Abbaszadeh, A. Kunz, G.A.H. Wetzelaer, J.J. Michels, N.I. Craciun, K. Koynov, I. Lieberwirth, P.W.M. Blom, Elimination of charge Carrier trapping in diluted semiconductors, Nat. Mater. 15 (2016) 628–633.
[30] N.E. Persson, P.H. Chu, M. McBride, M. Grover, E. Reichmanis, Nucleation, growth, and alignment of poly(3-hexylthiophene) nanofibers for high-performance OFETs, Acc. Chem. Res. 50 (2017) 932–942.
[31] S.A. Choulis, Y. Kim, J. Nelson, D.D.C. Bradley, M. Giles, M. Shkunov, I. McCulloch, High ambipolar and balanced Carrier mobility in regioregular poly(3-hexylthiophene), Appl. Phys. Lett. 85 (2004) 3890–3892.
[32] J. Zaumseil, H. Sirringhaus, Electron and ambipolar transport in organic field-effect transistors, Chem. Rev. 107 (2007) 1296–1323.